Available online at www.sciencedirect.com
ScienceDirect
International Journal of Heat and Mass Transfer 50 (2007) 1231–1237
International Journal of HEAT and MASS TRANSFER
www.elsevier.com/locate/ijhmt

Heat transfer performance in 3D internally finned heat pipe

Quan Liao [a], Tien-Chen Jen [a,*], Qinghua Chen [a], Longjian Li [b], Wenzhi Cui [b]

[a] *Mechanical Engineering Department, University of Wisconsin Milwaukee, Milwaukee, WI 53211, USA*
[b] *College of Power Engineering, Chongqing University, Chongqing 400044, China*

Received 15 June 2005; received in revised form 19 September 2006
Available online 13 November 2006

Abstract

An experimental study of heat transfer performance in 3D internally finned steel-water heat pipe was carried out in this project. All the main parameters that can significantly influence the heat transfer performance of heat pipe, such as working temperature, heat flux, inclination angle, working fluid fill ratio (defined by the evaporation volume), have been examined. Within the experimental conditions (working temperature 40 °C–95 °C, heat flux 5.0 kw/m^2–40 kw/m^2, inclination angle 2–90°), the evaporation and condensation heat transfer coefficients in 3D internally finned heat pipe are found to be increased by 50–100% and 100–200%, respectively, as compared to the smooth gravity-assisted heat pipe under the same conditions. Therefore, it is concluded that the special structures of 3D-fins on the inner wall can significantly reduce the internal thermal resistance of heat pipe and then greatly enhance its heat transfer performance.

Keywords: Heat pipe; Finned tube; Heat transfer enhancement; Heat transfer coefficient

1. Introduction

Heat pipe, which is a kind of high efficiency heat transfer device, has been used extensively in many industrial applications such as aerospace, power plants, air conditioning and refrigeration, pharmaceutical and chemical engineering [1,2]. It has been well recognized that the main challenges for the next generation of heat exchanger devices are the increasing demands of smaller size, lower weight, higher heat transfer efficiency and lower cost. Due to the skyrocketing oil prices, the ever-increasing pressure on energy cost has resulted in an urgent need for developing high efficiency heat exchanger devices [1].

It is well known that the two-phase flow and heat transfer exist in the heat pipe and it is the combination of evaporation and condensation phase change that makes heat pipes possess so many unique advantages, for example, nearly uniform temperature along the heat pipe axis, high equivalent axial thermal conductivity, and high reliability. According to different types of forces (for instance, gravitational force, centrifugal force, capillary force) that pump back the condensed working fluid from the condensation section to the evaporation section inside a heat pipe, the heat pipe can be classified as gravitational, centrifugal and capillary ones. Generally speaking, for capillary force assisted heat pipes, the capillary force is developed by different kinds of wick structure, such as powder sinter coating and small string bundle [1]. In those above wick structures, the powder sinter coating structure has proved to be the best way of providing much stronger capillary force than that of other wick structures. Although the high-temperature sintering process requires well-controlled temperature and pressure to create porous structures and this method can produce sufficient capillary force to make heat pipe work properly, the complicated manufacturing process has greatly limited extensive application in industrial settings [3], such as power plant heat exchanger and air-conditioning and refrigeration, except some special and high-value products, for example, laptops.

In order to further increase the rate of heat transfer and its performance of the heat-exchange devices, the proposed surface heat transfer enhancement technology can not only

* Corresponding author. Tel.: +1 414 229 2307; fax: +1 414 229 6958.
E-mail address: jen@cae.uwm.edu (T.-C. Jen).

0017-9310/$ - see front matter © 2006 Elsevier Ltd. All rights reserved.
doi:10.1016/j.ijheatmasstransfer.2006.09.010

Nomenclature

L_e	length of evaporation section of heat pipe, m	$T_{i,e}$	inner wall temperature of tube in the evaporation part, °C
L_a	length of adiabatic section of heat pipe, m	$T_{i,c}$	outer wall temperature of tube in the condensation part, °C
L_c	length of condensation section of heat pipe, m	T_v	working temperature of heat pipe, °C
G_{radial}	gap of the neighboring fins in radial direction, m	h_e	heat transfer coefficient of the evaporation part, kW/(m^2 °C)
G_{axial}	gap of the neighboring fins in axial direction, m	h_c	heat transfer coefficient of the condensation part, kW/(m^2 °C)
F_h	height of the fins, m	q_c	condensation heat flux, kW/m^2
D_{outer}	outer diameter of the heat pipe, m	q_e	evaporation heat flux, kW/m^2
D_{inner}	inner diameter of the heat pipe, m	R	volume ratio of working fluid in the evaporation part
Q_{total}	total heat added on the heat pipe, W	θ	inclined angle, °
U	voltage between the ends of the band heater, V		
I	current through the band heater, A		
A_e	outer surface area of the evaporation in the heat pipe, m^2		
A_c	outer surface area of the condensation in the heat pipe, m^2		

simplify the manufacturing processes of heat pipe, but also promote the heat transfer and, in some cases, supply sufficient capillary force to satisfy the need required by industrial standards [4,5]. The present project investigated the heat transfer performance of heat pipe with 3D internal fins.

2. Experimental schematic and measurements

As shown in Fig. 1, the experimental system consists of four parts: heating sub-system, cooling sub-system, inclination angle adjustment sub-system and measurement sub-system. Each part is described in detail as follows.

In the heating sub-system, to meet the requirement of uniform heat flux on the evaporation section, a flat band heater (whose cross section is $4 \times 0.2\,mm^2$) is closely placed and tightly wrapped around the outer surface of the evaporation section. In order to decrease the heat loss from the evaporation section to the ambient, a thermally insulating material (glass fiber mat), whose thermal conductivity is 0.043 W/(m K), is wrapped over the band heater with a thickness of 100 mm. Then, an electric transformer is used in the experiment to actively control the heat flux input on the heat pipe by varying the power input. When both the voltage and current, which are applied on the band heater, are measured, the power input for the heat pipe can be calculated directly.

The condensation section of heat pipe is included in the cooling sub-system, in which the cooling water with an adjustable flow rate and a constant inlet temperature is used to supply the condenser for the heat pipe. In the inclination angle adjustment sub-system, the heat pipe is installed on an angle-adjustable workbench, which can arbitrarily control the heat pipe's inclination angle from 0° to 90° with horizontal reference surface. Moreover, since the temperature is the key parameter that needs to be measured accurately in this experiment, the calibrated thermocouples are mounted on the outer surface of the heat pipe at evaporation, condensation and adiabatic sections, respectively. Finally, all of these thermocouples are

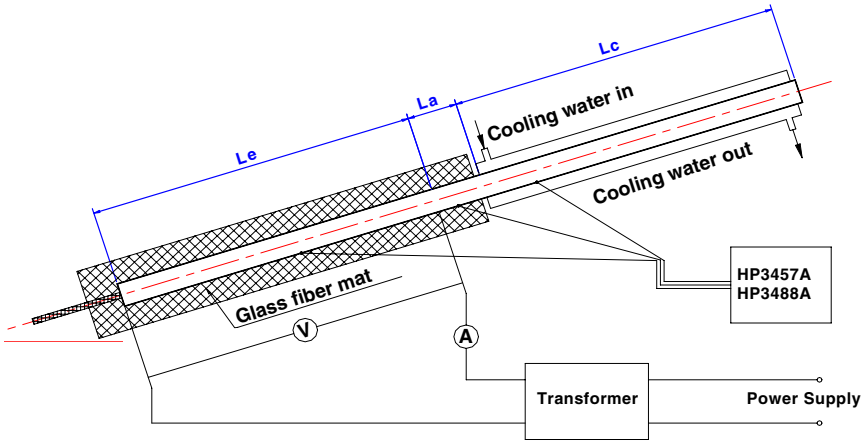

Fig. 1. Schematic of experimental system.

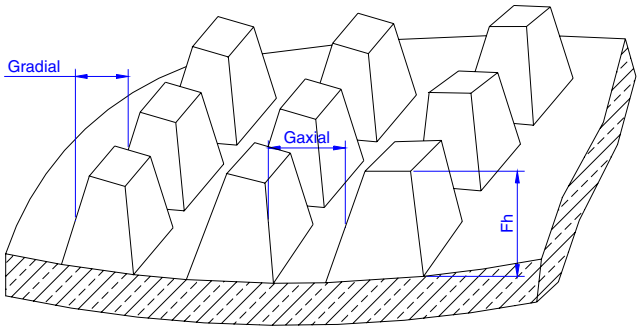

Fig. 2. Schematic of inner fin's structure.

Table 1
Geometric parameter of internal fins

Items	3D internally finned heat pipe	Smooth heat pipe
D_{outer} (mm)	27.0	27.0
D_{inner} (mm)	21.0	21.0
F_h (fin's height, mm)	0.15	–
G_{radial} (gap in radial direction, mm)	1.1	–
G_{axial} (gap in radial direction, mm)	1.0	–
Helical angle (°)	88.5	–
Top angle of fins (°)	45.0	–
Material	Carbon steel	Carbon steel

linked to the data acquisition system (HP3457A and HP3488A), through which the temperatures are automatically recorded.

The tested 3D internally finned heat pipe is made of carbon steel, with an outer diameter of 27 mm and an inner diameter of 21 mm. The pipe has a 700 mm long evaporation section, a 750 mm long condensation section and a 100 mm long adiabatic section. The inner structure of this tube is shown in Fig. 2 and the corresponding geometrical parameters and material of 3D inner fin and dimensions of smooth heat pipe are listed in Table 1. Since the insulating material is also wrapped at the adiabatic section with 100 mm thickness, the temperature measured by the thermocouple on the outer side of this section can be regarded as the heat pipe working temperature without significant error. Furthermore, before the data-usable experiments are performed, a calibration test for energy loss is first conducted by comparing the difference between the energy taken by the condensation section and the energy input in the evaporation section of heat pipe. The results demonstrate that the heat loss to the ambient is within 5.0% at room temperature 30 °C.

3. Data analysis and uncertainty

The instrumental errors involved in this experiment are shown in Table 2, and the error analysis in this paper is based on the policy of reporting uncertainties in experimental measurements and results [6,7]. According to these references, the experimental uncertainty is defined as follow:

Table 2
Uncertainty of the instruments

Parameters	Sensor	Error
Temperature (°C)	ϕ0.2 T type thermal couple	±0.15 °C
Inclined angle (°)	Inclined angle adjuster	±0.1°
Current (A)	Ampere meter	0.1%
Voltage (V)	Voltage meter	0.1%

For the variable R, $R = R(x_1, x_2, x_3, \ldots, x_n)$, the uncertainty is defined as

$$U_R = \{(B_R)^2 + (P_R)^2\}^{1/2} \tag{1}$$

where, the B_R and P_R are the bias limit and the precision limit of variable R, respectively. And they are defined as follows:

$$B_R = \left\{ \left(\frac{\partial R}{\partial x_1} Bx_1\right)^2 + \left(\frac{\partial R}{\partial x_2} Bx_2\right)^2 + \left(\frac{\partial R}{\partial x_3} Bx_3\right)^2 \cdots + \left(\frac{\partial R}{\partial x_n} Bx_n\right)^2 \right\}^{1/2} \tag{2}$$

$$P_R = \left\{ \left(\frac{\partial R}{\partial x_1} Px_1\right)^2 + \left(\frac{\partial R}{\partial x_2} Px_2\right)^2 + \left(\frac{\partial R}{\partial x_3} Px_3\right)^2 \cdots + \left(\frac{\partial R}{\partial x_n} Px_n\right)^2 \right\}^{1/2} \tag{3}$$

Generally, it is difficult to find the bias error for the specific experiment system because B_R is an estimation of the magnitude of the fixed, constant error. Therefore, in this paper we just consider the precision limit, P_R, and regard this error as the experimental uncertainty of the specific variable.

$$U_R = P_R \tag{4}$$

In this experiment, we regard the average temperature of the adiabatic section as the working temperature of the heat pipe (T_v) and all of the heat transfer coefficients (including the evaporation and condensation) are evaluated based on the following equations:

$$h_e = \frac{q_e}{T_{i,e} - T_v} = \frac{Q_{total}}{A_e \cdot (T_{i,e} - T_v)} = \frac{U \cdot I}{A_e \cdot (T_{i,e} - T_v)} \tag{5}$$

$$h_c = \frac{q_c}{T_{i,c} - T_v} = \frac{Q_{total}}{A_c \cdot (T_{i,c} - T_v)} = \frac{U \cdot I}{A_c \cdot (T_{i,c} - T_v)} \tag{6}$$

Therefore, the uncertainties for the heat transfer coefficients are:

$$\frac{U_{h_e}}{h_e} = \frac{P_{h_e}}{h_e} = \sqrt{\left(\frac{P_U}{U}\right)^2 + \left(\frac{P_I}{I}\right)^2 + \left(\frac{T_{i,e}}{T_{i,e} - T_v}\right)^2 \cdot \left(\frac{P_{T_{i,e}}}{T_{i,e}}\right)^2 + \left(\frac{T_v}{T_{i,e} - T_v}\right)^2 \cdot \left(\frac{P_{T_m}}{T_v}\right)^2} \tag{7}$$

$$\frac{U_{h_c}}{h_c} = \frac{P_{h_c}}{h_c} = \sqrt{\left(\frac{P_U}{U}\right)^2 + \left(\frac{P_I}{I}\right)^2 + \left(\frac{T_{i,c}}{T_{i,c} - T_v}\right)^2 \cdot \left(\frac{P_{T_{i,c}}}{T_{i,c}}\right)^2 + \left(\frac{T_v}{T_{i,c} - T_v}\right)^2 \cdot \left(\frac{P_{T_m}}{T_v}\right)^2} \tag{8}$$

where $T_{i,e}$ and $T_{i,c}$, which are calculated by Eq. (9), are the average temperatures of the inner side of the heat pipe at the evaporation and condensation section, respectively, and U and I are the voltage and current that are applied on the tested heat pipe.

Considering the thermal resistance of heat pipe's wall thickness in the radial direction, the temperature of the inner side of the tube is calculated in the following equation:

$$T_{w,in} = T_{w,out} - \frac{Q_{total}}{2\pi \cdot k_w \cdot l_i} \ln\left(\frac{D_{outer}}{D_{inner}}\right) \quad (9)$$

Finally, putting all the original experiment data and the uncertainties of instruments into Eqs. (7) and (8), the average uncertainties of the heat transfer coefficients (including evaporation and condensation) are ±5.1% and ±7.1%, respectively.

4. Results and discussion

As shown in Fig. 3, the evaporation heat transfer coefficient (h_e) vs. working temperature (T_v) in 3D internally finned heat pipes is illustrated with three different evaporation heat fluxes, i.e., 5.2 kw/m^2, 11.8 kw/m^2, and 14.2 kw/m^2. The inclination angle is 5°, and the fill ratio of the working fluid is 20%. It can be seen from this figure that at the same inclination angle (5°), the evaporation heat transfer coefficient increases as the working temperature increases [8]. It is also worth noting that at a high working temperature, the evaporation heat transfer coefficient will approach to a constant value when the evaporation heat flux is greater than a certain value.

Fig. 4 depicts the condensation heat transfer coefficient (h_c) vs. the working temperature with two different condensation heat fluxes, i.e., 18.0 kw/m^2 and 23.0 kw/m^2. The inclination angle at this condition is 12° and the fill ratio is 40%. In this figure, it is observed that the condensation heat transfer coefficient (h_c) increases with increasing working fluid temperature. At lower working temperatures (40 °C–70 °C), the rate of increase of condensation heat transfer coefficient is small. However, when the working temperature exceeds 70 °C, a significant increase in the rate of heat transfer coefficient is observed. That is because with the increase of working temperature, the physical properties in liquid and vapor phases are also changed correspondingly. For example, the thermal conductivity of working fluid (i.e., water) increased, hydrodynamic viscosity of the liquid decreased and vapor density increased, all of those have positive impacts on increasing the rate of heat transfer. One another factor that may affect the performance of the heat pipe is the presence of non-condensable gas. Even though the anti-corrosion and material compatibility between the working fluid and the heat pipe shell have been well considered before this experiment, there still exist some non-condensable gases, for example, air, hydrogen and other gases, which are generated by the chemical reaction between the working fluid and the metallic material of the tube when the heat pipe is at work or during the heat pipe assembling process. Therefore, when the working temperature is lower, the corresponding vapor pressure inside the heat pipe is also lower, and then the volume of non-condensable gases (or partial pressure) is much larger than that at a higher working temperature. Thus, the efficient condensation surface at a higher working temperature will be significantly greater than that at a lower working temperature, and the corresponding liquid film on the condensation surface at a higher working temperature will be much thinner than that at a lower working temperature. It is also worth noting that when the saturation temperature is lower than 60 °C–70 °C, the corresponding rate of increase of saturation pressure is much smaller than that when the temperature is between 70 °C and 100 °C (i.e., from a steam table). This explains the rapid increases in condensation heat transfer coefficient when the working temperature exceeds 70 °C. A final result is that the thermal resistance within the condensation section at the higher working temperature will be much smal-

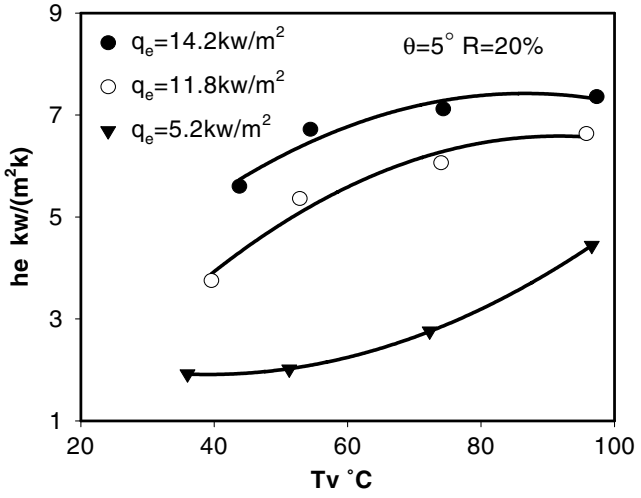

Fig. 3. Evaporation heat transfer coefficient vs. working temperature.

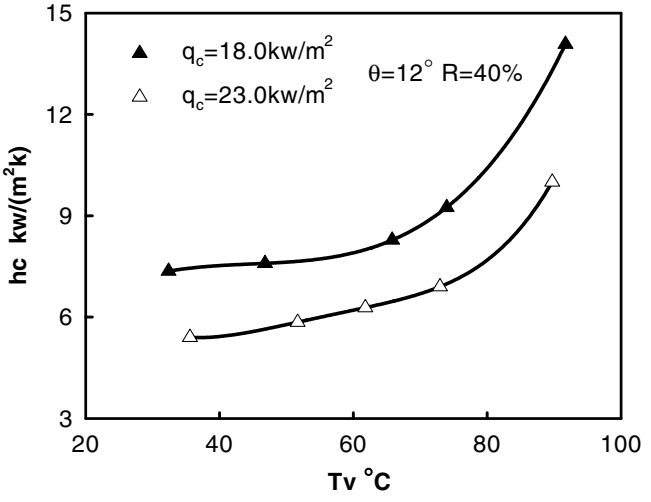

Fig. 4. Condensation heat transfer coefficient vs. working temperature.

ler than that at the lower working temperature. Due to the combination of those two factors, the condensation heat transfer coefficient is increased when the working temperature is increased.

Fig. 5 illustrates the effects of the inclination angle on the evaporation heat transfer coefficient in the 3D internally finned heat pipe at three different heat flux inputs, i.e., 5.1 kw/m^2, 8.9 kw/m^2, and 13.8 kw/m^2. The working temperature is fixed at 37.7 °C, and the fill ratio is 20%. It can be seen from the figure that the evaporation heat transfer coefficient increases when the inclination angle and/or the evaporation heat flux is increased. Note that when the inclination angle is very small (less than 2°), the dominant force to drive the condensed working fluid back to the evaporation section is only the capillary force. When the inclination angle is increased further, a significant increase is observed for the evaporation heat transfer coefficient. This is due to the assistance of gravitational force, besides the capillary force, which enables the working fluid to flow back to the evaporation section. Therefore, it greatly enhances the evaporation heat transfer coefficient. In addition, it is also interesting to note that when the inclination angle is greater than 12°, the rate of increase of the evaporation heat transfer coefficient becomes very small (i.e., the evaporation heat transfer coefficient is approaching a constant).

Fig. 6 demonstrates the effects of the inclination angle on the condensation heat transfer coefficient in the 3D internally finned heat pipe at three different heat flux inputs, i.e., 4.8 kw/m^2, 8.3 kw/m^2, and 12.9 w/m^2. The working temperature is fixed at 52.2 °C, and the fill ratio is 20%. Similar to Fig. 5, the condensation heat transfer coefficient increases when the inclination angle and/or the condensation heat flux is increased. It is worth noting that the influences of the inclination angle on the heat transfer performance in the condensation section lie in the flow patterns of condensed working fluid from the condensation to the evaporation section in the heat pipe, which are completely different at the different inclined angles. The flow patterns play an important role in the heat transfer performance of the heat pipe and the capillary capability of the wick structures in the heat pipe. When the inclination angle is very small (less than 2°), the flow pattern is very asymmetric due to the down pulling of the gravitational force. When the inclination angle is further increased, this asymmetric pattern is quickly reduced due to the interaction of the gravitational force and the capillary force along the circumference. Thus a more uniform distribution of working fluid film near the wall can be achieved, thus greatly enhancing the heat transfer performance of the heat pipe.

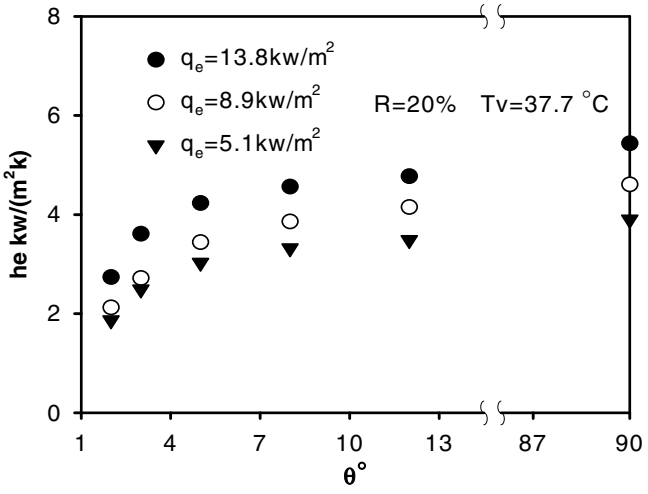

Fig. 5. Evaporation heat transfer coefficient vs. inclined angle.

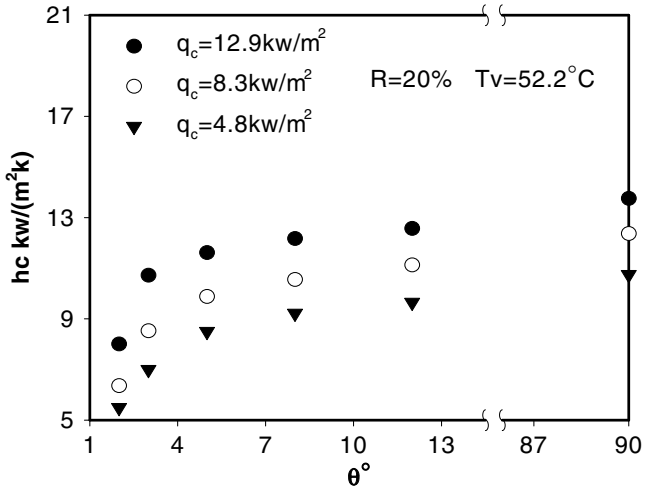

Fig. 6. Condensation heat transfer coefficient vs. inclined angle.

Comparisons of heat transfer coefficients (including evaporation and condensation section) between 3D internally finned heat pipe and smooth heat pipe are shown in Figs. 7 and 8. As shown in Fig. 7, the inclination angle is 8° and the fill ratio is 40%. Due to the difficulty of exactly controlling the working temperature of the heat pipe, the comparison between a 3D internally finned heat pipe with 91.8 °C working temperature and a smooth heat pipe with 94.6 °C working temperature is shown in Fig. 7. For both of those heat pipes, the evaporation heat transfer coefficient is increased when the evaporation heat flux is increased. Note that at a lower evaporation heat flux, a more significant increase for the evaporation heat transfer coefficient is observed, and the rate of increase reduces at higher evaporation heat flux. This is similar to that of the pool boiling cases. However, since the 3D internally finned heat pipe can provide many more nucleate sites, at the lower heat flux, the rate of increase of the heat transfer coefficient in the 3D heat pipe is significantly larger than that of the smooth heat pipe. Therefore, it can be seen from this figure that, compared with the smooth heat pipe, a significant increase for the evaporation heat transfer coefficient appears when the 3D internally finned heat pipe is used. And the increase of evaporation heat transfer coefficient is more than 100% at the lower heat flux condition (less than 10 kw/m^2), and about 50% at the higher heat flux condition. The significant enhancement of the heat transfer

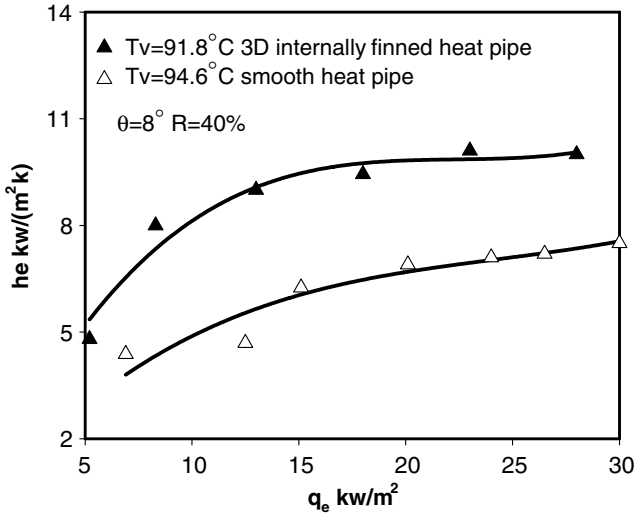

Fig. 7. Evaporation heat transfer coefficient vs. heat flux.

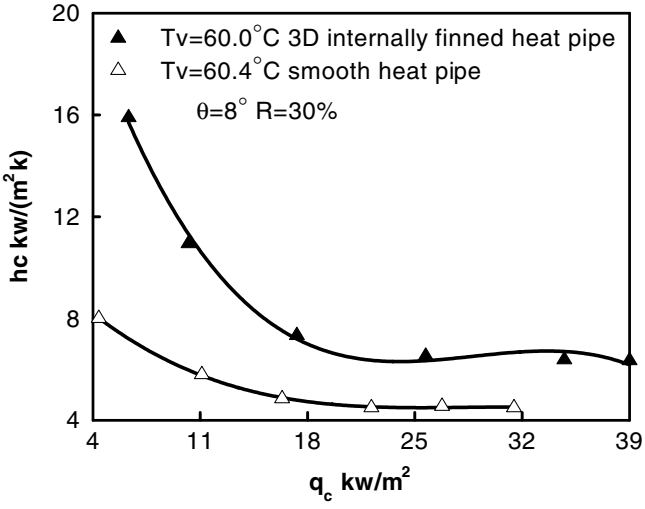

Fig. 8. Condensation heat transfer coefficient vs. heat flux.

coefficient is due to the special structure of the inner fin that makes the heat transfer performance in the 3D internally finned heat pipe much better than that in the smooth heat pipe because at the evaporation section, the 3D internal fin not only expands the real heat transfer surface area, but also increases the boiling nucleate sites, thus greatly enhancing the heat transfer.

Fig. 8 presents the comparison of the condensation heat transfer coefficient between the 3D internally finned heat pipe with the smooth heat pipe at different condensation heat flux inputs. The inclination angle is chosen to be 8°, and the fill ratio is 30%. The working temperature for the 3D internally finned heat pipe is 60.0 °C and for the smooth heat pipe is 60.4 °C. In this figure, it can be seen that the rate of increase of the condensation heat transfer coefficient for the 3D internally finned heat pipe is 100–200%, compared with the smooth heat pipe. A significant difference is observed for the condensation heat transfer coefficient when the condensation heat flux is small (i.e., less than 11 kw/m^2). This can be explained as follows: at the condensation section, when the heat flux is low, all the internal fins are exposed in the working fluid vapor and between the two neighboring fins the capillary force makes the condensed liquid thickness much thinner than that in the smooth heat pipe. Therefore, at the small heat flux the 3D internally heat pipe has much better condensation heat transfer performance than that of the smooth heat pipe. However, as the heat flux further increases, the returning liquid thickness on the inner wall of the tube increases. The advantage of capillary force for redistribution of the working fluid has been diminished due to the smaller height between the working liquid and fin. This advantage will disappear when all the internal fins are completely submerged in the condensed working fluid. Therefore, it will cause the thermal resistance in the condensation section of the heat pipe to increase and the condensation heat transfer performance will be greatly decreased, as shown in this figure.

Although the fill ratio is not very high (just 20%, 30% and 40% of the evaporation volume, respectively), it can still clearly show that the fill ratio does not play an important role in influencing the heat transfer performance in the 3D internally finned heat pipe [9]. This is because the structure of the internal fins makes the working fluid so uniformly distributed in the evaporation section that the fill ratio involved in this experiment is sufficient to wet all the evaporation surface area, thus guaranteeing that the heat pipe works well.

5. Conclusions

This paper describes the heat transfer performance of the 3D internally finned heat pipe with different main parameters, such as working temperature, heat flux, fill ratio and inclination angle. The experimental data show that this kind of new 3D internally finned heat pipe has more advantages than the traditional smooth gravity-assisted heat pipe because the special structures of 3D internal fins on the inner side of the heat pipe can significantly reduce the heat pipe internal thermal resistance and therefore greatly enhance its heat transfer performance. Within the experimental conditions, the evaporation and condensation heat transfer coefficients of the 3D internally finned heat pipe are increased 50–100% and 100–200%, respectively, compared with the smooth heat pipe.

In this project, the small inclined angle (2–13°) of 3D internally finned heat pipe has been studied in detail. The experimental data showed that the inclination angle plays an important role on the heat transfer performance (including condensation and evaporation) of the 3D internally finned heat pipe, especially when the inclination angle is less than 13°. When the inclination angle is increased over 13°, however, its effect is no longer significant.

Acknowledgements

Dr. Tien-Chien Jen, Mr. Quan Liao and Mr. Qinghua Chen would like to acknowledge the partial financial support from NSF GOALI grant DMII-9908324 for this work.

References

[1] S.W. Chi, Heat Pipe Theory and Practice, Hemisphere Publishing Corporation, 1976.
[2] D. Scott, P.E. Garner, Heat Pipes for Electronics Cooling Applications, Electronics Cooling Magazine, Thermacore Inc., 1996.
[3] M. Xin, Fundamental and Applications of Heat Pipe, Science and Technology Publishing Corporation, Chongqing, China, 1977.
[4] M. Xin, J. Zhou, G. Zhang, Q. Chen, W. Cui, Boiling heat transfer of R134a in the horizontal 3D internally finned tube, J. Thermal Phys. 22 (1) (2001).
[5] Q. Chen, W. Cui, J. Zhou, G. Zhang, Condensation heat transfer of superheated R134a vapor in the horizontal 3D internally finned tube, J. Thermal Phys. 21 (4) (2000).
[6] J.H. Kim, T.W. Simon, R. Viskanta, Journal of Heat Transfer policy on reporting uncertainties in experimental measurements and results, (Editorial), J. Heat Transfer 115 (1) (1993) 5–6.
[7] R.J. Moffat, Using uncertainty analysis in the planning of an experiment, ASME J. Fluids Eng. 107 (2) (1985) 173–178.
[8] K. Ling, Experiments of Wind Cooler for Generator with Heat Pipe, Master thesis of Chongqing University, Chongqing, China, November 1994.
[9] S. Xing, Heat transfer performance of heat pipe with small inclined angle, Master Thesis of Chongqing University, Chongqing, China, January 1989.